# Tracking of Vehicle Motion on Highways and Urban Roads Using a Nonlinear Observer

Woongsun Jeon, Ali Zemouche and Rajesh Rajamani

Abstract—This paper focuses on the development and use of a nonlinear observer for tracking of vehicle motion trajectories while using a radar or laser sensor. Previous results on vehicle tracking have typically used an interacting multiple model filter that needs different models for different modes of vehicle motion. This paper uses a single nonlinear vehicle model that can be used for all modes of vehicle motion. Previous nonlinear observer design results from literature do not work for the nonlinear system under consideration due to the wide range of operating conditions that need to be accommodated. Hence, a new nonlinear observer design technique that utilizes better bounds on the coupled nonlinear functions in the dynamics is developed. The exponential stability of the observer is established using Lyapunov techniques. The observer design with the developed technique is then implemented in both simulations and experiments. Experimental results show that the observer can simultaneously and accurately estimate longitudinal position, lateral position, velocity and orientation variables for the vehicle from radar measurements. Results are presented both for tracking of vehicle maneuvers on highways and of maneuvers on urban roads at traffic intersections where turns and significant changes in vehicle orientation can

*Index Terms*—Nonlinear observer, vehicle motion estimation, vehicle tracking.

## I. INTRODUCTION

VEHICLE motion tracking is an important problem that is frequently encountered in autonomous driving, as well as in collision avoidance and adaptive cruise control (ACC) applications [1-5]. There has been significant recent interest in the autonomous control of vehicles [6-8, 17-18], but the topic of estimating the trajectories of other vehicles on a road in order to track them or avoid conflicts with them has not been sufficiently addressed. Collision avoidance and ACC systems typically use radar or laser sensors for measuring distances and azimuth angles [1-5] to vehicles. With such sensors, radial distances and azimuth angles can be measured.

In the case of vehicles in urban traffic, including vehicles at traffic intersections, the radar-measured variables are inadequate in order to fully predict the trajectories of vehicles. Both lateral and longitudinal distances and orientation of the vehicles are needed in order to accurately predict vehicle

motion and provide appropriate warnings or automated driving actuation. Previous work in vehicle tracking has typically utilized interacting multiple model (IMM) filters for estimation of vehicle trajectories [9-11]. The models used in the IMM filter typically include a "straight line driving" model and a "constant turn rate" model. Each model can be used for its respective driving scenario and is not applicable for the other scenario.

This paper develops a vehicle tracking algorithm that uses a single model to represent all possible vehicle motions involving both longitudinal and lateral maneuvers. By using a single vehicle model, stability of the state observer can be guaranteed and the real-time computational effort in estimating trajectories of multiple vehicles on the road is reduced in comparison with the IMM approach. The observer gains are obtained by off-line computation while the IMM approach uses multiple models and recomputes gains in real-time.

Since the proposed vehicle model is nonlinear, an effective nonlinear observer design technique is required to ensure an exponentially stable observer. Two nonlinear observer design techniques from literature that are designed for bounded Jacobian systems are first used in an attempt to obtain a stable observer. However, their design procedures fail to yield stable observer gains for this application, due to infeasibility of the associated Linear Matrix Inequalities (LMIs). A new nonlinear observer design technique suitable for this application is therefore developed. The stability of the observer is proved, and an observer gain for the vehicle model application is obtained for a larger operating range than the previous observer design techniques from literature. The advantage of the developed observer is the increased feasibility of a solution due to less conservative LMIs in the observer design equation.

The developed observer is used to track the lateral and longitudinal positions and orientation of a vehicle in both simulations and experiments. A radar sensor that measures radial distance and azimuth angle is used as the measurement unit. Vehicles maneuvers that include straight driving cars, a lane change maneuver, a double lane change maneuver, cross traffic driving at a traffic intersection, and a left turn maneuver are considered in this paper. Thus, the observer works for both highway driving and urban traffic that includes intersections.

The outline of the rest of the paper is as follow: In the next

This research was supported in part by a research grant from the National Science Foundation (NSF Grant PFI-1631133).

Woongsun Jeon and Rajesh Rajamani are with the Department of Mechanical Engineering, University of Minnesota, Twin Cities, Minneapolis, MN 55455 USA (e-mail: jeonx121@umn.edu; rajamani@umn.edu, TEL: 612-626-7961).

Ali Zemouche is with the University of Lorraine, CRAN CNRS UMR 7039, 54400 Cosnes et Romain, France. (e-mail: ali.zemouche@univ-lorraine.fr).

section, the proposed nonlinear observer design technique is presented. In Section III, we propose a single vehicle model that can represent both longitudinal and lateral maneuvers, and discuss vehicle motion tracking using the vehicle model and developed observer. Then, in Section IV and V, the proposed vehicle motion tracking algorithm is validated in both simulations and experiments. Conclusions are presented in Section VI.

## II. NONLINEAR OBSERVER DESIGN

## A. Problem Statement

Before introducing the vehicle tracking problem, we start by proposing a new LMI-based nonlinear observer design method. This methodology provides less conservative LMI conditions for observer design than those existing in the literature.

We consider the class of nonlinear systems described by

$$\dot{x} = f(x, u) 
y = Cx$$
(1)

where  $x \in R^n$  is the state vector,  $u \in R^m$  is the input vector and  $y \in R^p$  is the output vector.  $C \in R^{p \times n}$  is a matrix of appropriate dimensions.  $f(x,u): R^n \times R^m \to R^n$  is a vector of differentiable nonlinear functions.

The following Luenberger-like observer will be studied:

$$\dot{\hat{x}} = f(\hat{x}, u) + L(y - C\hat{x}) \tag{2}$$

where L is the observer gain matrix to be designed such that exponential convergence of the estimation error  $\tilde{x} = x - \hat{x}$  towards zero is obtained.

## B. Existing Nonlinear Observer Design Methods

Previous researchers have developed nonlinear observer design techniques suitable for bounded Jacobian systems using the mean value theorem [12, 13]. These studies define and use Jacobian bounds based on element-wise minimum and maximum values of the Jacobian. By considering the nonlinear system and observer described in (1) and (2), the following results can be summarized from the existing methods in literature.

*Lemma 1:* Differential Mean Value Theorem using Canonical Basis [12, 13].

Let  $f(x): \mathbb{R}^n \to \mathbb{R}^n$  be a function continuous on  $[a,b] \in \mathbb{R}^n$  and differentiable on convex hull of the set (a,b) with Lipschitz continuous gradient. For  $s_1, s_2 \in [a,b]$ , there exists  $z \in (a,b)$  such that

$$f(s_2) - f(s_1)$$

$$= \left(\sum_{i,j=1}^{n,n} e_n(i)e_n^T(j)\frac{\partial f_i}{\partial x_j}(z_i)\right)(s_2 - s_1)$$
(3)

where  $e_n(i) = (0, \dots, 0, 1, 0, \dots, 0)^T \in \mathbb{R}^n$  is a vector of the canonical basis of  $\mathbb{R}^n$  with 1 at  $i_{th}$  component.

**Theorem 1** [12]: If an observer gain matrix L can be chosen such that

$$P(\overline{H}_{ij}^{max}) + (\overline{H}_{ij}^{max})^{T} P - C^{T} L^{T} P - PLC < 0$$

$$P(\overline{H}_{ij}^{min}) + (\overline{H}_{ij}^{min})^{T} P - C^{T} L^{T} P - PLC < 0$$

$$P > 0$$
(4)

 $\forall i = 1, \dots, n$ , and  $\forall j = 1, \dots, n$ , where

1)  $h_{ij}^{max} \ge \max(\partial f_i/\partial x_i)$  and  $h_{ij}^{min} \le \min(\partial f_i/\partial x_i)$ ;

- 2)  $H_{ij}^{max} = e_n(i)e_n^T(j)h_{ij}^{max}$  and  $H_{ij}^{min} = e_n(i)e_n^T(j)h_{ij}^{min}$ ;
- 3)  $Z_H = n \times n$  is the state scaling factor, n being dimension of the state vector;
- of the state vector; 4)  $\overline{H}_{ij}^{max} = Z_H H_{ij}^{max}$  and  $\overline{H}_{ij}^{min} = Z_H H_{ij}^{min}$ ;

then this choice of L leads to asymptotically stable estimates by the observer for the system.

**Theorem 2** [13]: The observer estimation error converges exponentially towards zero if there exist matrices  $P = P^T > 0$  and R of appropriate dimensions such that the following LMIs are feasible:

$$A^{T}(\vartheta)P + PA(\vartheta) - C^{T}R - R^{T}C < 0$$

$$\forall \vartheta \in v_{H_{n,n}}$$
(5)

where

$$A(\vartheta) = \sum_{i,j=1}^{n,n} e_n(i) e_n^T(j) \frac{\partial f_i}{\partial x_j}(z_i)$$
 (6)

and the domain  $v_{H_{n,n}}$  is defined by

$$\begin{aligned} v_{H_{n,n}} &= \{\vartheta = (\vartheta_{11}, \cdots, \vartheta_{1n}, \cdots, \vartheta_{nn}) | \vartheta_{ij} \\ &\in \{h_{ii}, \overline{h}_{ii}\} \} \end{aligned} \tag{7}$$

$$\underline{h}_{ij} = \min(\partial f_i / \partial x_j) \text{ and } \overline{h}_{ij} = \max(\partial f_i / \partial x_j)$$
 (8)

When these LMIs are feasible, the observer gain L is given by  $L = P^{-1}R^{T}$ .

However, these methods do not work for the application of vehicle motion tracking considered in this paper. Specifically, the LMI toolbox in MATLAB fails to provide a feasible solution for the multiple LMIs that need to be simultaneously satisfied in both Theorems 1 and 2. It should be noted that an observer gain (and an associated *P* matrix) that satisfy multiple LMIs need to be obtained in both methods. Hence, a new nonlinear observer design method suitable for the vehicle tracking application is presented herein.

## C. Analysis of Domain of Jacobian Matrix

In order to further motivate the new nonlinear observer design method, we investigate the domain of the Jacobian matrix and the reason for failure of the observer design methods from [12] and [13].

From (4) in *Theorem 1* and (8) in *Theorem 2*, it is obvious that the element-wise minimum and maximum values of the Jacobian are used to satisfy stability conditions of the observers. However, this approach is likely to be conservative, especially when there are coupled terms in the Jacobian matrix of the nonlinear function. For example, let us consider the following nonlinear system:

$$\dot{x} = f(x) \\
v = Cx$$
(9)

where

$$f(x) = \begin{bmatrix} x_3 \cos x_4 \\ x_3 \sin x_4 \\ 0 \\ 0 \end{bmatrix}, C = \begin{bmatrix} 1 & 0 & 0 & 0 \\ 0 & 1 & 0 & 0 \end{bmatrix}$$
 (10)

This nonlinear system is similar to the vehicle tracking application. The Jacobian matrix of the nonlinear function  $x_3 cos x_4$  is

$$\frac{\partial f_1}{\partial x} = \begin{bmatrix} 0 & 0 & \cos x_4 & -x_3 \sin x_4 \end{bmatrix} \tag{11}$$

Using element-wise inequalities with the assumption  $5 \le x_3 \le 15$  and  $-\pi/3 \le x_4 \le \pi/3$ , it can be concluded that the

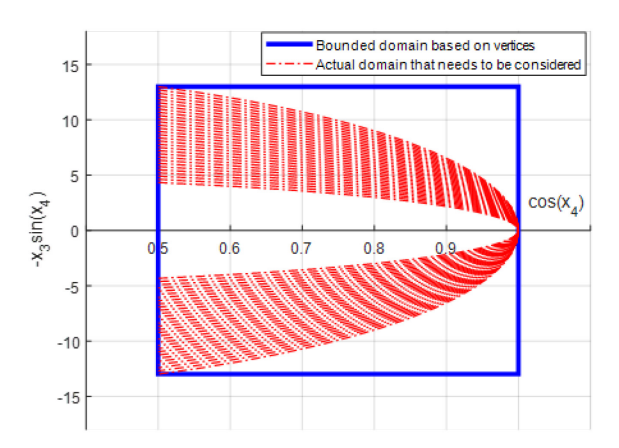


Fig. 1. Illustration of domains from Jacobian of nonlinear function.

Jacobian of the nonlinear function is in a bounded domain defined by vertices:

$$v_1 = (0.5, 12.99), v_2 = (1, 12.99),$$
  
 $v_3 = (1, -12.99), v_4 = (05, -12.99)$ 

However, designing the observer to be stable over this entire domain is challenging. In fact, some parts of the domain do not need to be considered. For instance, the vertex  $v_3$  spans from  $x_4 = 0$  for the cosine function and  $x_4 = \pi/3$  for the sine function in (11) which are contradictory to each other. The sine and cosine functions are never going to be maximum at the same values of their identical arguments. Fig. 1 illustrates both the bounded domain based on the vertices, and the actual domain that needs to be considered of the Jacobian. It is true that the Jacobian always evolves within the bounded domain of the vertices. However, it is possible that the bounded domain based on the vertices becomes too conservative as the Jacobian of the system has many coupled terms.

## D. Nonlinear Observer

In this section, we present a modified nonlinear observer design method for the nonlinear system described in the previous three sections.

**Theorem 3:** Consider the nonlinear system (1) and observer form (2). If there exist matrices  $P \ge I$  and R of appropriate dimensions such that the following problem is solvable:

$$\min \gamma$$
 subject to (12)

$$P \ge I \tag{13}$$

$$\begin{bmatrix}
P & R^{T} \\
R & \gamma I
\end{bmatrix} \ge 0$$

$$A(\xi, u)^{T} P + PA(\xi, u) - C^{T} R - R^{T} C$$
(14)

$$A(\xi, u) \cdot P + PA(\xi, u) - C \cdot R - R \cdot C + 2\alpha P \le 0,$$

$$\forall u \in u_{grid}, \forall \xi \in \xi_{grid}$$

$$(15)$$

where 
$$A(\xi, u) = \frac{\partial f}{\partial x}(\xi, u), \xi \in \mathbb{R}^n$$

then, the observer gain L is given by

$$L = P^{-1}R^T \tag{16}$$

and with this value of the observer gain, the estimation error of the observer (2) converges exponentially towards zero.

*Proof*: Let the Lyapunov function candidate for observer design be defined as  $V = \tilde{x}^T P \tilde{x}$  where  $P = P^T > 0$  and  $P \in \mathbb{R}^{n \times n}$ . For exponential stability, we will require that the derivative of V satisfies the following differential inequality:

$$\dot{V} \le -2\alpha V \tag{17}$$

where  $\alpha$  is a positive constant. The inequality (17) implies the exponential stability condition [14]:

$$||x(t) - \hat{x}(t)|| \le \kappa ||x(0) - \hat{x}(0)||e^{-\alpha t}$$
 (18)

where  $\kappa$  is a positive constant. From the Lyapunov function candidate, the derivative of V can be represented as

$$\dot{V} = -\tilde{x}^T \{ (LC)^T P + P(LC) \} \tilde{x} + 2\tilde{x}^T P \delta f$$
 (19)

where  $\delta f = f(x, u) - f(\hat{x}, u)$ . The difference of the functions  $\delta f$  can be presented by using the integral form of the mean value theorem [15] for vector functions:

$$\delta f = \left( \int_0^1 \frac{\partial f}{\partial s} \Big|_{s=x+\eta(\hat{x}-x)} d\eta \right) (x - \hat{x})$$
 (20)

Then, we can write

$$\dot{V} + 2\alpha V 
= \int_{0}^{1} \left( \tilde{x}^{T} \left\{ \left[ \frac{\partial f}{\partial s} \right]_{s=x-\eta(x-\hat{x})} - LC \right]^{T} P \right. 
\left. + P \left[ \frac{\partial f}{\partial s} \right]_{s=x-\eta(x-\hat{x})} - LC \right] + 2\alpha P \left\{ \tilde{x} \right\} d\eta$$
(21)

Using the notation

$$\xi \triangleq x - \eta(x - \hat{x}) \tag{22}$$

$$A(\xi, u) \triangleq \frac{\partial f}{\partial s}(\xi, u) \tag{23}$$

(21) becomes

$$\dot{V} + 2\alpha V 
= \int_0^1 (\tilde{x}^T \{ [A(\xi, u) - LC]^T P 
+ P[A(\xi, u) - LC] + 2\alpha P \} \tilde{x}) d\eta$$
(24)

Since  $\xi$  varies with the value of x and  $\hat{x}$ , A is an unknown and continuously time varying matrix. From (24), (17) is satisfied when following condition is satisfied:

$$(A(\xi, u) - LC)^T P + P(A(\xi, u) - LC) + 2\alpha P$$

$$< 0$$
(25)

By introducing a new variable  $R = L^T P$ , (25) can be expressed as

$$A(\xi, u)^T P + PA(\xi, u) - C^T R - R^T C + 2\alpha P$$

$$\leq 0$$
 (26)

Since  $\xi$  and u vary infinitely in a given set, (26) gives us infinitely many LMIs. This can be reduced to a finite number of LMIs using gridding techniques. We fix a finite subset of the  $\xi$  and u within its bounds such that

$$u_{grid} \in \{u_1, \dots, u_N\}$$
  
$$\xi_{grid} \in \{\xi_1, \dots, \xi_N\}$$
 (27)

It is noted that the dimension of the grid is proportional to the number of varying variables in  $\xi$  and u. Also, the points of the finite subset need to be chosen sufficiently dense so that solving LMIs for the finite subset is equivalent to satisfying the original stability condition. Therefore, the observer design condition (15) can be obtained.

Unfortunately, the observer gain L can be arbitrarily large, if only the design condition (26) is utilized. Hence, we use the following additional specification [16] for L. If (15) with  $P = P^T > 0$  has a solution for P and R, the following size condition must be satisfied for  $\gamma$  sufficiently large:

$$||L|| \le \sqrt{\gamma} \tag{28}$$

This means that  $\sqrt{\gamma}$  is an upper bound on the norm of the gain L. Without loss of generality, we can assume that  $P \ge I$ . Since  $L = P^{-1}R^T$  and  $\gamma$  is sufficiently large, the condition (28) becomes

$$L^T L \le L^T P L = R P^{-1} R^T \le \gamma I \tag{29}$$

From this, we obtain

$$\gamma I - RP^{-1}R^T \ge 0 \tag{30}$$

Using the Schur complement, (30) can be represented as (14).

#### III. VEHICLE MOTION TRACKING PROBLEM

# A. Proposed Vehicle Motion Model

Previous models used for tracking of vehicle motion in active safety or autonomous driving applications have primarily involved longitudinal motion variables (and sometimes additional lateral position variables) of the vehicle. For instance, a popular approach for radar based vehicle tracking consists of an interacting multiple model filter with two models – a "constant velocity" model and a "nearly coordinated turn" model [19]. The state vector is assumed to be

$$x = [X \quad Y \quad v \quad \theta \quad \omega] \tag{31}$$

where (X,Y), v,  $\theta$ , and  $\omega$  are the target vehicle position in Cartesian coordinates, speed, orientation, and turn rate in the sensor body frame. The discrete-time state space equation for the constant velocity model is given by

$$x_{k+1} = \begin{bmatrix} X + vT\cos\theta \\ Y + vT\sin\theta \\ v \\ \theta \\ 0 \end{bmatrix}_{\nu} + w_{v,k}$$
 (32)

where  $w_{v,k}$  is process noise sequence represented by zero mean gaussian noise. The discrete-time state space equation for the nearly coordinated turn model is given by

$$=\begin{bmatrix} X + \frac{2v}{\omega} \left\{ \sin\left(\frac{\omega T}{2}\right) \cos\left(\theta + \frac{\omega T}{2}\right) \right\} \\ Y + \frac{2v}{\omega} \left\{ \sin\left(\frac{\omega T}{2}\right) \sin\left(\theta + \frac{\omega T}{2}\right) \right\} \\ v \\ \theta + \omega T \\ \omega \end{bmatrix}_{k} + w_{t,k}$$
(33)

where  $w_{t,k}$  is process noise sequence represented by zero mean gaussian noise.

It should be noted that the constant velocity model is applicable to straight line motion and the coordinated turn model only applies while turning. Neither model can be used for both scenarios and the coordinated turn model, in fact, becomes singular when the rotation rate becomes zero.

Another disadvantage of the above approach is that all the three degrees of freedom have independent unknown inputs – lateral, longitudinal and orientation variables are all driven by unknown terms.

This paper proposes the use of a single nonlinear model that encompasses both straight line and turning motions. Considering only planar motion for the vehicle, the motion of the vehicle can be described by X, Y and  $\psi$  as shown in Fig. 2. X and Y are coordinates of longitudinal and lateral locations of

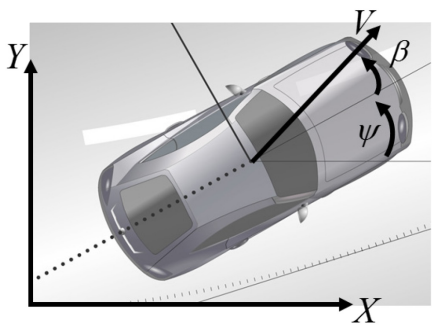


Fig. 2. Vehicle motion model.

the vehicle with respect to the sensor (radar or LIDAR) location, and  $\psi$  is orientation angle of the vehicle with respect to the X axis, i.e., the orientation angle is with respect to the sensor (ego vehicle). Assuming that the slip angles at the tires are zero (but the slip angle of the vehicle itself is not zero), the model equations can be described by

$$\dot{X} = V\cos(\psi + \beta) \tag{34}$$

$$\dot{Y} = V \sin(\psi + \beta) \tag{35}$$

$$\dot{\psi} = \frac{V \cos(\beta)}{l_f + l_r} \tan(\delta_f)$$
 (36)

$$\beta = \tan^{-1} \left( \frac{l_r \tan(\delta_f)}{l_f + l_r} \right) \tag{37}$$

and

$$\dot{V} = a \tag{38}$$

where V is the speed of the vehicle,  $\beta$  is the slip angle of the vehicle.  $l_f$  and  $l_r$  are the distances from the center of gravity of the vehicle to the front and rear wheelbases of the vehicle,  $\delta_f$  is steering angle of front wheel and a is the acceleration of the vehicle.  $\delta_f$  and a are unknown inputs. More understanding of the nonlinear vehicle model can be found by reading [20].

The location of the vehicle is assumed to be measured by using a radar or LIDAR sensor. Therefore, the output equations can be written as

$$y = \begin{bmatrix} X \\ Y \end{bmatrix} = Cx \tag{39}$$

where

$$C = \begin{bmatrix} 1 & 0 & 0 & 0 \\ 0 & 1 & 0 & 0 \end{bmatrix}$$
, and  $x = [X \ Y \ V \ \psi]^T$  (40)

Then, the form of the system and output equations above is the same as the form of (1) used for the nonlinear observer development.

It should be noted that the "zero slip angle at the tires" assumption could be avoided, and a model that assumes the tire force as a function of the slip angle could be utilized. However, such a model becomes a function of a large number of tire and vehicle parameters. Since the vehicle that is encountered and is being tracked is unknown, the values of these parameters cannot be known. Hence, the above model is more appropriate, in spite of the zero-slip-at-tire assumption.

It should be noted that the sum  $l_f + l_r$  is constant for each vehicle, even if exact center of gravity of the vehicle is not known. This sum is assumed to be 2.8 meters for all vehicles. While the actual length may have erros of 10 - 15% from this value, this does not lead to much error in the orientation estimates. One reason for this is the dependence of  $\dot{X}$  and  $\dot{Y}$  on

the  $\psi$  in the dynamic model. This enables  $\psi$  to be estimated correctly.

It should be noted that this model has two unknown inputs (steering angle  $\delta_f$  and longitudinal acceleration a). Both of these unknown inputs can be assumed to be constants (or slowly changing) and equations with their derivates as zero can be appended to the dynamic model used for tracking.

# B. Observer Design for Vehicle Motion Tracking

The nonlinear observer is designed by the method proposed in section II. D with the nonlinear vehicle motion model (34) – (38). First, note that

$$f(x,u) = \begin{cases} V\cos(\psi + \beta) \\ V\sin(\psi + \beta) \\ a \\ \frac{V\cos(\beta)}{l_f + l_r} \tan(\delta_f) \end{cases}$$
(41)

Hence,  $A(\xi, u)$  in (15) can be computed from the Jacobian of the vehicle motion model and is found to be:

$$A(\xi, u) = \begin{bmatrix} 0 & 0 & \cos(\psi + \beta) & -V\sin(\psi + \beta) \\ 0 & 0 & \sin(\psi + \beta) & V\cos(\psi + \beta) \\ 0 & 0 & 0 & 0 \\ 0 & 0 & \frac{\cos(\beta)}{l_f + l_r} \tan(\delta_f) & 0 \end{bmatrix}$$
(42)

The Jacobian in (42) has 3 time-varying variables: V,  $\delta_f$  and  $\psi$  over which gridding is required. We need to define the operating ranges of these variables. Then, a finite 3-dimensional grid is constructed, consisting of the entire range of operating conditions.  $A(\xi, u)$  is evaluated at each grid point on this 3-demensional grid. Finally, we solve (12) – (16) for the observer gain using the LMI toolbox in MATLAB, so as to obtain a single observer gain valid for all values of  $A(\xi, u)$ .

Preliminary results were presented by us on an observer for vehicle motion on just highways in a conference publication [21]. Since only highway driving was involved, the operating range of  $\psi$  was limited. In this paper, we deal with both highway and urban road driving involving a very large operating range for  $\psi$  and hence the need for a switched gain observer. It turns out that a constant gain matrix cannot be used for the entire operating range  $0 \le \psi \le 2\pi$ . However, stable observers can be designed for more limited operating ranges, if the  $0 \le \psi \le 2\pi$  region is divided into 4 sub-regions. Using the observer gains obtained from these 4 sub-regions, a switched gain approach is needed to cover the full range  $0 \le \psi \le 2\pi$ . It should be noted that the new observer design technique developed in this paper based on a grid still yields exponential stability for a much larger operating range than the existing observer design methods [12, 13] described earlier. The observer design method using Theorem 1 fails to provide an observer gain, and the observer design method using *Theorem* 2 provides an observer gain for very limited operating range:  $-19^{\circ} \le \psi \le 19^{\circ}$  with  $3m/s \le V \le 15m/s$ , and  $-10^{\circ} \le$  $\delta_f \leq 10^{\circ}$ .

As a result, the proposed observer works for most vehicle motions: straight driving, lane change, double lane change, and cross traffic motions without using a switched gain approach.

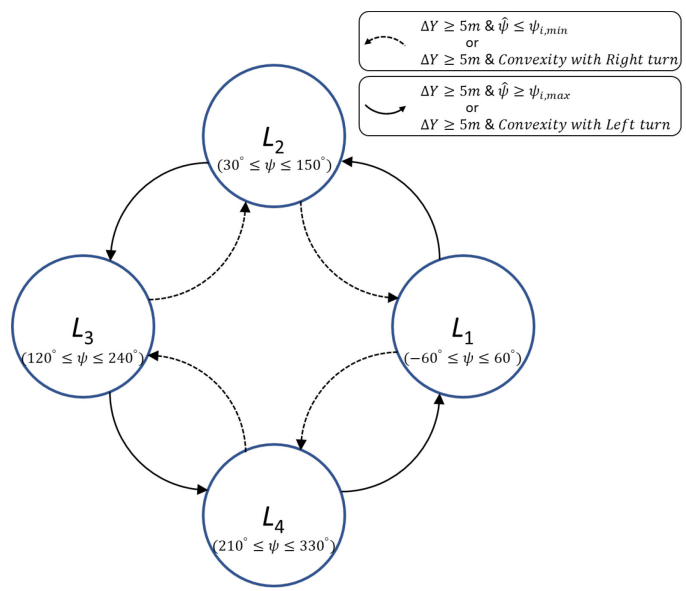


Fig. 3. Finite state machine for gain switching.

Only left and right turn vehicle motions are required to use a switched gain approach.

## C. Switched Gain Approach

By using the proposed nonlinear observer design method in *Theorem 3*, four constant gain matrices  $L_1$ ,  $L_2$ ,  $L_3$  and  $L_4$  can be obtained for use in the following operating ranges respectively:

- 1)  $-60^{\circ} \le \psi \le 60^{\circ}$ ,
- 2)  $30^{\circ} \le \psi \le 150^{\circ}$ ,
- 3)  $120^{\circ} \le \psi \le 240^{\circ}$ ,
- 4)  $210^{\circ} \le \psi \le 330^{\circ}$ ,

with  $3m/s \le V \le 15m/s$ , and  $-10^{\circ} \le \delta_f \le 10^{\circ}$ . By using proper initial target vehicle orientation and switching the gain properly, the observer can estimate vehicle motion for the entire operating range.

Fig. 3 shows a finite state machine for gain switching. Each finite state is for a different operating range  $\psi_{i,min} \leq \psi \leq \psi_{i,max}$  and uses a different observer gain  $L_i$  for  $i=1,\cdots,4$ . Since vehicle motion is nonholonomic, there are only two possible options for switching from current state. For example, if initial orientation of vehicle (heading angle) is within  $-60^{\circ} \leq \psi \leq 60^{\circ}$ , the vehicle cannot suddenly be oriented in  $120^{\circ} \leq \psi \leq 240^{\circ}$  without going through either  $30^{\circ} \leq \psi \leq 150^{\circ}$  or  $210^{\circ} \leq \psi \leq 330^{\circ}$ .

The stability of the hybrid observer in Fig. 3 consisting of 4 different constant observer gain regions needs to be considered. It should be noted that inside each region, a single observer gain is used and exponential stability is guaranteed using the Lyapunov function analysis of *Theorem 3*. However, the 4 regions may use 4 different values of the matrix P > 0 in their individual Lyapunov functions. The stability of the overall switched system can be guaranteed if the system satisfies a minimum dwell time constraint in each region, according to results from hybrid system theory [22]. The minimum dwell time in region j when switching from region i to region j needs to be greater than T where T is the amount of time needed for  $V_i(x(t+T)) < V_i(x(t))$ . This minimum dwell time guarantees

global asymptotic stability. This result can be understood as follows: In each individual region, the estimation error  $\tilde{x}$  keeps decreasing due to the Lyapunov exponentially stable design. In switching between regions, the P matrix may be different in the two regions. However, if the system remains in the same region for a minimum dwell time, the error will become smaller than the initial value at the time the region was entered (due to local exponential stability). Thus, if the system is constrained to remain in one region for a minimum dwell time, the value of the Lyapunov function after the dwell time in region j is less than its value in region i at the time the switch from i to j occurred. This guarantees overall asymptotic stability [22].

In the case of the observer design application for the 4 separate regions of  $\psi$ , the values of  $\psi$  at which the region is entered and at which it switches back are different (as shown in Fig. 3). This hysteresis between entering and switching back ensures that the minimum dwell time constraint is met.

Initial conditions of the vehicle motion are decided based on an initial small number of measurements. Predominantly, initial target vehicle orientation is one of four cases:  $0^{\circ}$  or  $180^{\circ}$  when the target vehicle is driving longitudinally from the sensor orientation point of view, and  $90^{\circ}$  or  $270^{\circ}$  when the target vehicle is driving laterally from the sensor orientation point of view. First, rough relative velocity between target vehicle and sensor platform can be calculated based on initial couple of position measurements and its time information. By using the relative velocities  $(V_{r,x}, V_{r,y})$ , an angle can be calculated as

$$\psi_r = \tan^{-1}(V_{r,y}/V_{r,x}) \tag{43}$$

From the calculated angle, it is possible to determine whether or not the vehicle constitutes cross-traffic. By comparing with the velocity of sensor platform, the moving direction of target vehicle is obtained and the vehicle orientation  $\psi_0$  is selected among the four orientations. Therefore, initial target vehicle orientation can be determined without ambiguity.

This method provides initial conditions that are close enough to the true values to choose correct initial state (gain) and to make the observer converge quickly.

In this paper, two methods A and B are proposed for the gain switching in the observer to estimate vehicle motion for the entire range  $0 \le \psi \le 2\pi$ . In practice, common maneuvers such as straight line motion and lane change motion do not need gain switching. However, left or right turning motion at intersections requires gain switching. For instance, consider a typical left turn vehicle motion in which the orientation of the vehicle evolves from  $0^{\circ}$  to  $90^{\circ}$ . When  $\psi$  exceeds  $60^{\circ}$ , gain switching should be conducted from  $L_1$  to  $L_2$  since  $L_1$  works only for the operating range  $-60^{\circ} \le \psi \le 60^{\circ}$ . As we can see, the observer gain needs to switch based on the value of  $\psi$ . However,  $\psi$  is not a directly measurable variable. Therefore, it is important to develop methods that detect vehicle turn motion without knowing  $\psi$ . It should be noted that lane change maneuvers should be distinguished from turn maneuvers because a lane change maneuver has a smaller orientation change and does not need gain switching.

Method A: The first method utilizes estimated orientation  $\psi$  and lateral movement of target vehicle. State (gain) is switched

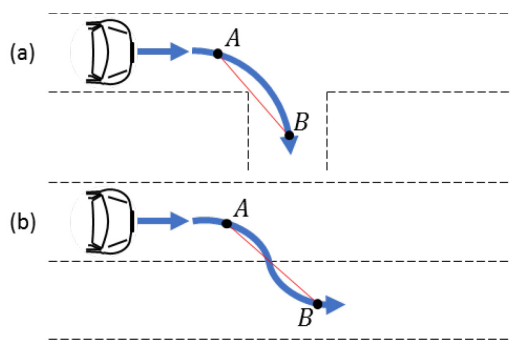


Fig. 4. Illustration of how *Method B* distinguishes between (a) Left turn maneuver, and (b) Lane change maneuver.

to next available region based on the operating range if

- 1) Lateral movement  $\Delta Y$  exceeds 5m, and
- 2)  $\hat{\psi}$  is exceeding upper (or lower) bound of operating range of  $\psi$  at the current state, as shown in Fig. 3.

The value of 5m is used as a threshold because typical road width and turning radius are of the order of 4m and 5m respectively. This method works well in practice since relatively good initial condition can be obtained as described earlier and the initial condition makes estimates converge quickly to the true values. Furthermore, each operating range for an observer gain is overlapped with nearby regions by 30 degrees. This overlap and the proposed switching rule prevent repeated switching behavior. For example, the value of  $\psi$  at which the switch from regon 1 to 2 occurs is different from the value of  $\psi$  at which the reverse switch from region 2 to 1 occurs. The specific values are specified in the transition rules for switching between the different regions. Importantly, the overlap improves robustness of the switching against estimation error. A switched gain still makes the observer stable if the true orientation is within the overlapped range. Once a vehicle is in

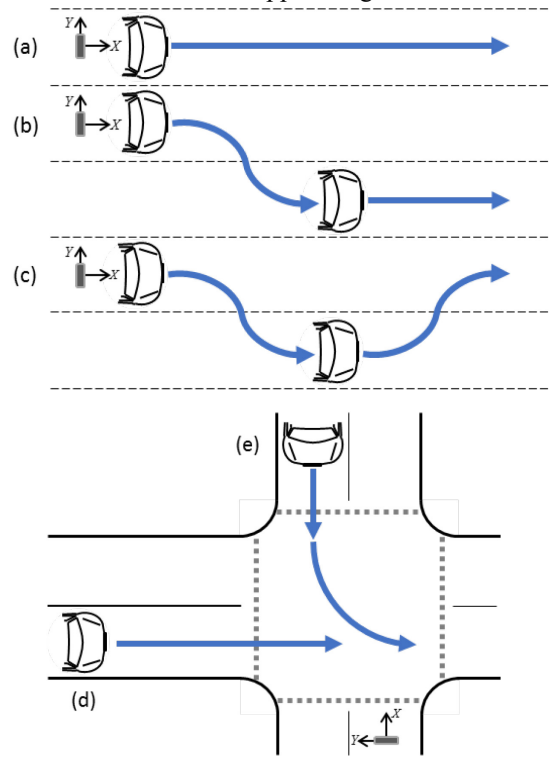


Fig. 5. Vehicle motions: (a) Straight driving, (b) Lane change, (c) Double lane change, (d) Cross traffic and (e) Left turn vehicle motions.

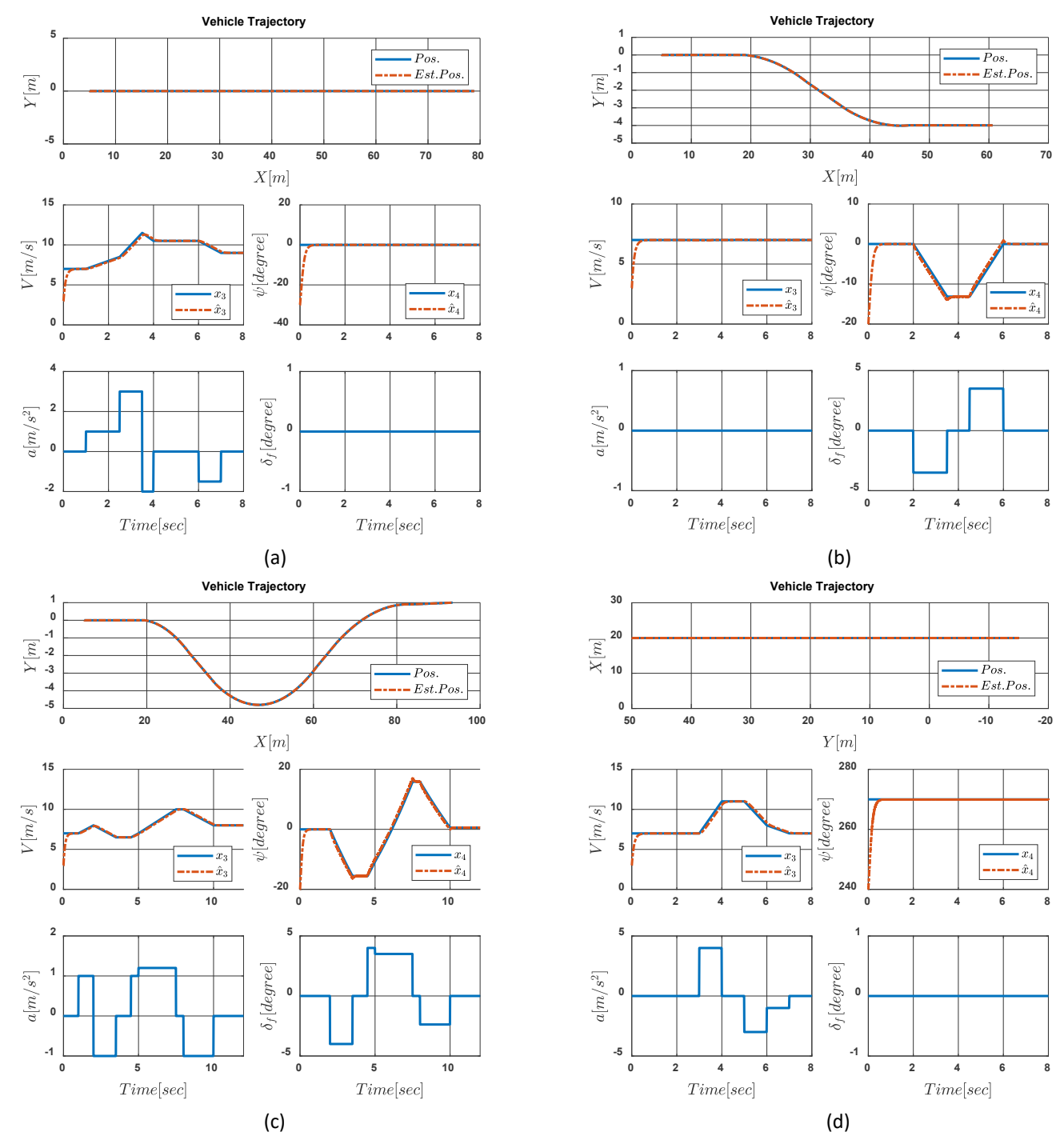


Fig. 6. Simulation results of (a) Straight driving maneuver, (b) Lane change maneuver, (c) Double lane change maneuver, and (d) Cross traffic maneuver.

straight line motion mode, i.e., estimated orientation of the vehicle is near 0°, 90°, 180° or 270°, the reference lateral position of the vehicle is updated for next switching.

*Method B*: Switching can be determined by only using measured information. The procedure is as follows:

- 1) Initiate collection of position measurements when  $\Delta Y$  exceeds 0.3m (point A in Fig. 4).
- 2) Store the measurement until  $\Delta Y$  exceeds 5m (point B in Fig. 4), and then go to the next step.
- 3) Check the convexity of polygon drawn by the line AB and measurements (curve AB), as shown in Fig. 4.
- 4) If the polygon is convex and the curve AB is on the

downstream side of the line, state (gain) is switched to next available state based on the turning direction, as shown in Fig. 3.

Fig. 4 shows the difference between lane change motion and turning motion based on the proposed method. It is obvious that the polygon from turning motion is convex and the polygon from lane change motion cannot be convex. Once lateral movements are within the threshold 0.3m for an adequate time window, reference lateral position of the vehicle is updated for next switching.

Finally, it should be noted that while the inputs of steering angle and acceleration in the vehicle model were assumed to be

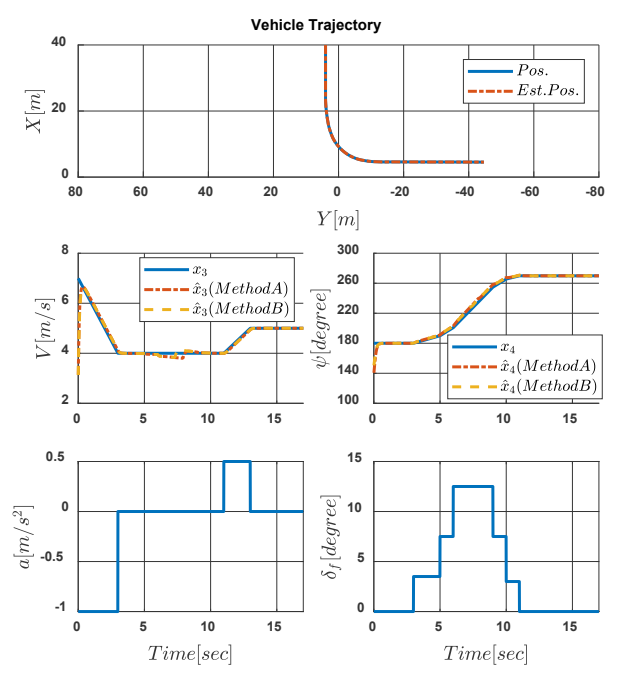


Fig. 7. Simulation results of left turn maneuver.

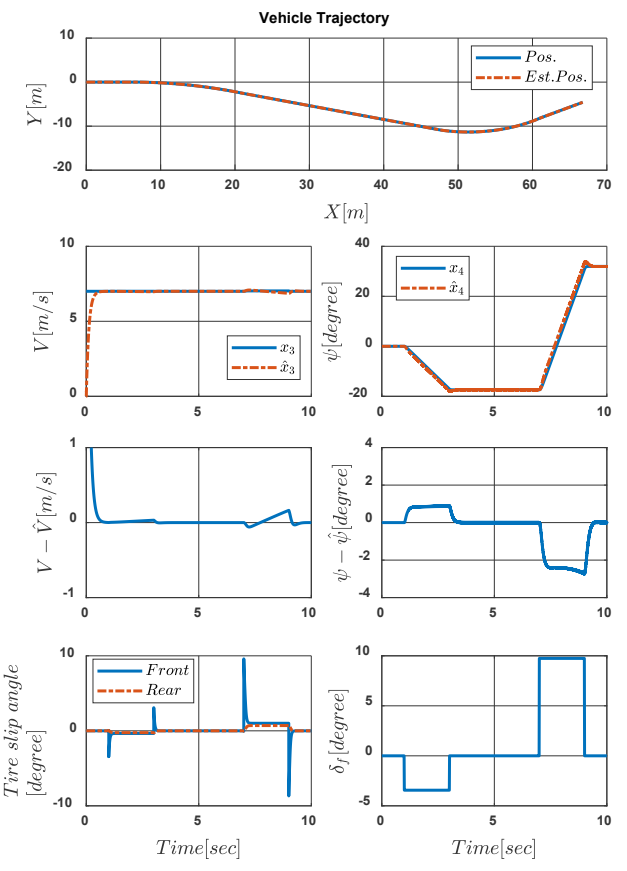
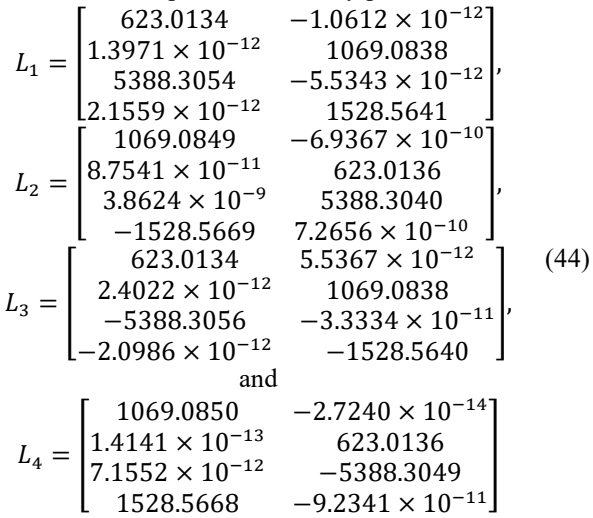


Fig. 8. Simulation results of the performance in the presence of tire slip angles. constant, the influence of non-zero inputs on estimation error can be calculated using Lyapunov analysis [13]. A bounded non-zero input for an exponentially stable observer will result in a bounded estimation error, as shown in [13]. The bound on the estimation error can be designed to be small by using a LMI-based  $H_{\infty}$  design condition, as was done in [13].

## IV. SIMULATION RESULTS

The nonlinear observer for vehicle motion tracking described in the previous section has first been evaluated using Matlab simulations. Simulation studies are conducted for various scenarios of highway vehicle motion: straight driving, lane change, and double lane change motion as shown in Fig. 5 (a), (b), and (c). Also, cross traffic and left turn vehicle at intersections, as shown in Fig. 5 (d) and (e) are simulated, as scenarios specific local driving.  $l_f$  and  $l_r$  are assumed to be 1.35m and 1.45m. A sensor is assumed to be located at the origin of the coordinate system in Fig. 5. The trajectories of the vehicle are generated by using the nonlinear vehicle motion model. Each trajectory and the inputs for the trajectories are shown in Fig. 6 and 7.

The observer gains are calculated by using the four operating conditions with the exponential stability parameter  $\alpha = 0.3$ :



As described earlier, relatively good initial conditions can be obtained by using first few samples from sensor measurements. However, in this simulation study, we intentionally use inaccurate initial conditions for the velocity and orientation to show the convergence of the observer.

The estimation results using the nonlinear observer with a single gain are shown in Fig. 6. Only small estimation errors are presented during transient periods. Also, Fig. 7 shows estimation results of a left turn vehicle. The switched gain approach is utilized to track vehicle motion over a large operating range. Both methods A and B conduct gain switching properly and track vehicle motion successfully. Overall, the proposed nonlinear observer provides good performance for vehicle motion tracking. The estimates of the vehicle motion converge to the true vehicle motion, even with unknown steering and acceleration inputs.



Fig. 9. (a) Delphi ESR, and (b) Experimental setup using a tripod.

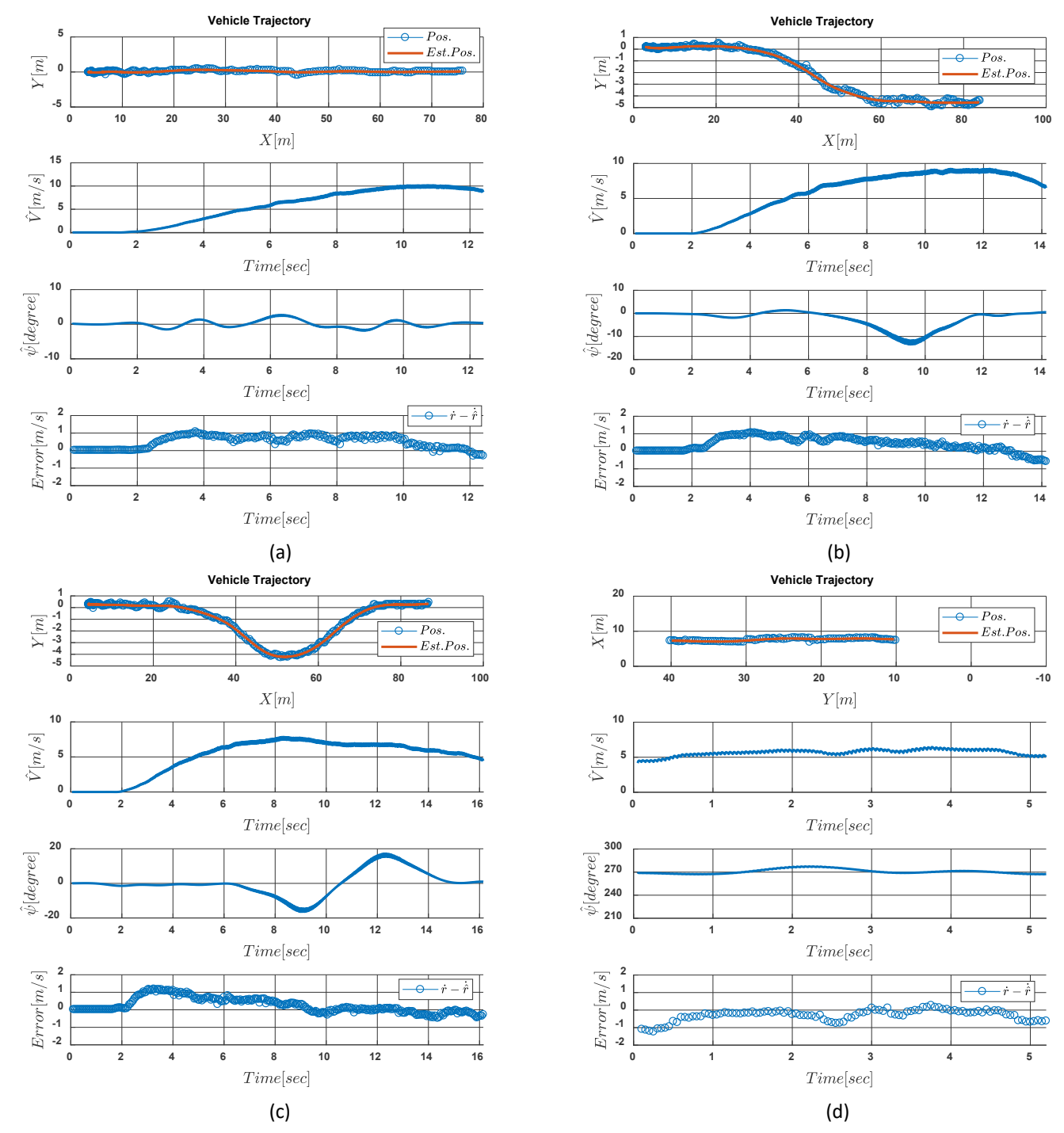


Fig. 10. Experimental results of (a) Straight driving maneuver, (b) Lane change maneuver, (c) Double lane change maneuver, and (d) Cross traffic maneuver.

Simulation studies in the presence of large tire slip angles are also conducted. As shown in Fig. 8, two steering actions are considered to evaluate the performance of the proposed observer in the presence of large tire slip angles. A vehicle first changes the orientation using a small steering action, and then suddely change the vehicle orientation to the opposite direction using a large steering action. Large tire slip angles (traction limited event) occur due to the abrupt large steering action. In the simulation studies, Dugoff's tire model [20] is utilized. Simulation results in Fig. 8 with a nolinear tire force model show that while the observer continues to track lateral and longitudinal positions very accurately, the estimation of vehicle

orientation experiences larger errors in the presence of large tire slip angles.

## V. EXPERIMENTAL RESULTS

Experiments are conducted to validate the proposed nonlinear observer design in situations corresponding to all the five scenarios in Fig. 5, of i) Straight Driving, ii) Lane Change, iii) Double Lane Change, iv) Cross Traffic, and v) Left Turn maneuvers. The Delphi Electronically Scanning Radar (ESR) shown in Fig. 9 is used for the experimental evaluation. The radar was mounted on a tripod, and measured all vehicle

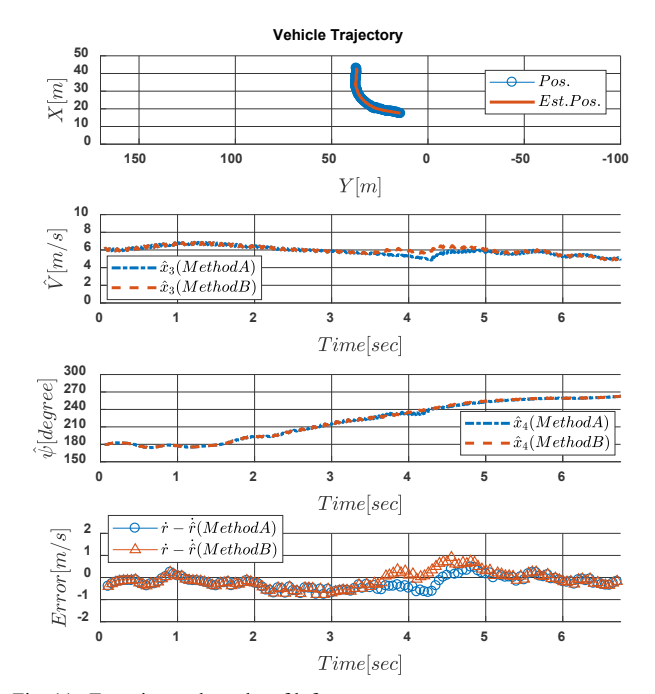


Fig. 11. Experimental results of left turn maneuver.

positions in the experiment. The radar provides vehicle radial position information within 174 meters of maximum range and 45 degrees of maximum field of view [23]. A low pass filter is used to smoothen the radar's vehicle position data, before supplying it to the observer. Also, the radial velocity of the target can be obtained from the radar. However, we only use the velocity information as a reference to compare with estimates, for the validation of the proposed nonlinear observer.

The observer gains are obtained by using the four operating conditions with the exponential stability parameter  $\alpha=0.1$ . Initial conditions are calculated by using first two samples from the radar measurement. Fig. 10 and 11 show the experimental results for the five scenarios. It is seen that the proposed nonlinear observer can estimate the vehicle motion based on radar measurements, without knowing the steering and acceleration of the vehicle. The estimates from the experimental data provide very reasonable evolutions of the orientation of the vehicle which are quite similar as the orientation results from the simulations. Also, the radial velocity of the target vehicle measured by the radar can be used to evaluate the performance of the proposed observer. The estimated radial velocity of the target vehicle can be computed by using estimates:

$$\dot{\hat{r}} = \frac{\hat{x}\hat{V}\cos(\hat{\psi}) + \hat{Y}\hat{V}\sin(\hat{\psi})}{\sqrt{\hat{x}^2 + \hat{Y}^2}} \tag{45}$$

The error between the radial velocity and estimated radial velocity is shown in Fig 10 and 11. Mostly, the error is less than

TABLE I Error of Radial Velocity Estimate

Vehicle maneuver	Max. Error [m/s]	RMSE [m/s]
Straight driving	1.0827	0.6045
Lane change	1.0659	0.5571
Double lane change	1.1917	0.4867
Cross traffic	1.2715	0.4532
Left turn (Method A)	0.7654	0.3638
Left turn (Method B)	0.9111	0.3759

1m/s. Detailed values of the maximum and root mean square error (RMSE) are shown in Table I.

## VI. CONCLUSIONS

A vehicle tracking algorithm that uses a single model to represent all possible vehicle motions is presented in this paper. By using a single vehicle model, nonlinear observer design techniques can be utilized. The developed nonlinear observer guarantees stability of the estimates over large operating regions and requires less real-time computational effort in estimating trajectories of multiple vehicles on the road, compared to a traditional interacting multiple model filter.

The developed observer is used to track vehicle motion including the lateral and longitudinal positions, velocity and yaw orientation of a vehicle. Simulation results were presented to show the performance of the developed observer in the application of vehicle motion tracking. Experimental results were also presented using a radar sensor that measures polar distance and azimuth angle as the measurement unit. Both simulations and experiments show excellent results in vehicle motion tracking on vehicle maneuvers including straight driving cars, a lane change maneuver, a double lane change maneuver, a cross traffic maneuver, and a left turn maneuver.

The developed observer successfully estimates vehicle motion for a larger operating range than existing observer techniques from literature. One disadvantage of the proposed method is the high computational effort in computing a gain using the gridding technique. However, it should be noted that this computation is done offline and not in real-time. Future work will include further development of the vehicle tracking observer design method to reduce the high offline computational burden in computing the observer gain.

#### REFERENCES

- [1] G. R. Widmann, M. K. Daniels, L. Hamilton, L. Humm, B. Riley, J. K. Schiffmann, D. E. Schnelker, and W. H. Wishon, "Comparison of lidar-based and radar-based adaptive cruise control systems," No. 2000-01-0345. SAE Technical Paper, 2000.
- [2] R. Abou-Jaoude, "ACC radar sensor technology, test requirements, and test solutions," in *IEEE Transactions on Intelligent Transportation Systems*, vol. 4, no. 3, pp. 115-122, Sept. 2003.
- [3] A. Petrovskaya, and S. Thrun, "Model based vehicle detection and tracking for autonomous urban driving," in *Autonomous Robots*, vol. 26, issue 2-3, pp. 123-139, April 2009.
- [4] C. Urmson, J. Anhalt, D. Bagnell, C. Baker, R. Bittner, M. N. Clark, J. Dolan et al., "Autonomous driving in urban environments: Boss and the urban challenge," *Journal of Field Robotics*, vol. 25, issue 8, pp. 425-466, August 2008.
- [5] A. Mukhtar, L. Xia and T. B. Tang, "Vehicle detection techniques for collision avoidance systems: A Review," *IEEE Transactions* on *Intelligent Transportation Systems*, vol. 16, no. 5, pp. 2318-2338, Oct. 2015.
- [6] E. Kayacan, H. Ramon and W. Saeys, "Robust Trajectory Tracking Error Model-Based Predictive Control for Unmanned Ground Vehicles," *IEEE/ASME Transactions on Mechatronics*, Vol. 21, No. 2, pp. 806-814, April 2016.
- [7] H. An, J. Liu, C. Wang and L. Wu, "Approximate Back-Stepping Fault Tolerant Control of the Flexible Air-Breathing Hypersonic

- Vehicle," *IEEE/ASME Transactions on Mechatronics*, Vol. 21, No. 3, June 2016.
- [8] C. Shen, Y. Shi and B. Buckham, "Integrated Path Planning and Tracking Control of an AUV: A Unified Receding Horizon Optimization Approach," *IEEE/ASME Transactions on Mechatronics*, Vol. 22, No. 3, pp. 1163-1173, June 2017.
- [9] W. Jeon and R. Rajamani, "Rear Vehicle Tracking on a Bicycle Using Active Sensor Orientation Control," in *IEEE Transactions* on *Intelligent Transportation Systems*, vol. 19, no. 8, pp. 2638-2649, Aug. 2018.
- [10] N. Kaempchen, K. Weiss, M. Schaefer and K. C. J. Dietmayer, "IMM object tracking for high dynamic driving maneuvers," Proceedings of *IEEE Intelligent Vehicles Symposium*, 2004, pp. 825-830, 2004.
- [11] Y. Kang, C. Roh, S. B. Suh and B. Song, "A Lidar-Based Decision-Making Method for Road Boundary Detection Using Multiple Kalman Filters," in *IEEE Transactions on Industrial Electronics*, vol. 59, no. 11, pp. 4360-4368, Nov. 2012.
- [12] G. Phanomchoeng, R. Rajamani and D. Piyabongkarn, "Nonlinear Observer for Bounded Jacobian Systems, With Applications to Automotive Slip Angle Estimation," in *IEEE Transactions on Automatic Control*, vol. 56, no. 5, pp. 1163-1170, May 2011.
- [13] A. Zemouche, M. Boutayeb and G. I. Bara, "Observers for a class of Lipschitz systems with extension to H∞ performance analysis," in *Systems & Control Letters*, vol. 57, issue 1, pp. 18-27, 2008.
- [14] H. K. Khalil, Nonlinear Systems, Prentice Hall, Upper Saddle River, NJ, USA, 3rd edition, 2002.
- [15] J.M. Ortega, W.C. Rheinboldt, Iterative Solution of Nonlinear Equations in Several Variables, SIAM, Philadelphia, 2000
- [16] B. Açıkmeşe, and M. Corless, "Observers for systems with nonlinearities satisfying incremental quadratic constraints," in *Automatica*, vol. 47, issue 7, pp. 1339-1348, July 2011.
- [17] R. Wang, C. Hu, F. Yan and M. Chadli, "Composite Nonlinear Feedback Control for Path Following of Four-Wheel Independently Actuated Autonomous Ground Vehicles," in *IEEE Transactions on Intelligent Transportation Systems*, Vol. 17, No. 7, pp. 2063-2074, July 2016.
- [18] S. K. Kommuri, M. Defoort, H. R. Karimi and K. C. Veluvolu, "A Robust Observer-Based Sensor Fault-Tolerant Control for PMSM in Electric Vehicles," in *IEEE Transactions on Industrial Electronics*, vol. 63, no. 12, pp. 7671-7681, Dec. 2016.
- [19] X. Rong Li, and V. P. Jilkov, "Survey of maneuvering target tracking. Part I. Dynamic models," in *IEEE Transactions on Aerospace and Electronic Systems*, vol. 39, no. 4, pp. 1333-1364, Oct 2003.
- [20] R. Rajamani, Vehicle dynamics and control, Springer Science & Business Media, 2011.
- [21] W. Jeon, A. Zemouche and R. Rajamani, "Nonlinear Observer for Vehicle Motion Tracking," *Proceedings of the 2018 American Control Conference (ACC)*, Milwaukee, WI, 2018.
- [22] P. Colaneri, J.C. Geromel and A. Astolfi, "Stabilization of Continuous-time Switched Nonlinear Systems," Systems & Control Letters, Vol. 57, pp. 95-103, 2008.
- [23] Delphi. ESR [Online]. Available: https://www.delphi.com/manufacturers/auto/safety/active/electronically-scanning-radar.



Woongsun Jeon received the B.S. and M.S. degrees in mechanical engineering from Yonsei University, Seoul, Korea in 2010 and 2012, respectively. Currently he is working toward the Ph.D. degree in mechanical engineering at the University of Minnesota, Twin Cities, Minneapolis, MN, USA. His research interests include

sensing, estimation, and control systems.



Ali Zemouche received his Ph.D. degree in automatic control in 2007, from the University Louis Pasteur, Strasbourg, France, where he held post-doctorate degree from October 2007 to August 2008. Dr. Zemouche joined, as Associate Professor, the Centre de Recherche en Automatique de Nancy (CRAN UMR

CNRS 7039) at the Université de Lorraine, since september 2008. He held an academic position at Inria – Saclay (EPI DISCO) from September 2016 to August 2017. His research activities include nonlinear systems, state observers, observerbased control, time-delay systems, robust control, and application to real-world models. Dr. Zemouche is currently associate editor in international journals: SIAM Journal of Control and Optimization, European Journal of Control, Cogent Engineering, DESIGNS (MDPI Journal). He is also a member of the Conference Editorial Board of IEEE Control Systems Society and IFAC TC2.3 (Non-Linear Control Systems).



Rajesh Rajamani obtained his M.S. and Ph.D. degrees from the University of California at Berkeley in 1991 and 1993 respectively and his B.Tech degree from the Indian Institute of Technology at Madras in 1989. Dr. Rajamani is currently Professor of Mechanical Engineering at the University of Minnesota. His active

research interests include sensors and estimation systems for mechanical engineering applications.

Dr. Rajamani has co-authored over 135 journal papers and is a co-inventor on 13 patents/ patent applications. He is the author of the popular book "Vehicle Dynamics and Control" published by Springer Verlag. Dr. Rajamani has served as Chair of the IEEE Technical Committee on Automotive Control and on the editorial boards of the IEEE Transactions on Control Systems Technology, the IEEE/ASME Transactions on Mechatronics, and the IEEE Control Systems Magazine. Dr. Rajamani is a Fellow of ASME and has been a recipient of the CAREER award from the National Science Foundation, the 2001 Outstanding Paper award from the journal *IEEE Transactions on Control Systems Technology*, the Ralph Teetor Award from SAE, and the 2007 O. Hugo Schuck Award from the American Automatic Control Council.